Proceedings of the ASME 2013 International Design Engineering Technical Conferences and Computers and Information in Engineering Conference
IDETC/CIE 2013
August 4-7, 2013, Portland, Oregon, USA

DETC2013-13637

DESIGN AND MEASUREMENT ERROR ANALYSIS OF A LOW-FRICTION, LIGHTWEIGHT LINEAR SERIES ELASTIC ACTUATOR

Bryce Lee
Virginia Tech
Blacksburg, Virginia, USA

Viktor Orekhov
Virginia Tech
Blacksburg, Virginia, USA

Derek Lahr MS
Virginia Tech
Blacksburg, Virginia, USA

Dennis Hong PhD
Virginia Tech
Blacksburg, Virginia, USA

ABSTRACT

Series elastic actuators (SEAs) have many benefits for force controlled robotic applications. Placing an elastic member in series with a rigid actuator output enables more-stable force control and the potential for energy storage while sacrificing position control bandwidth. This paper presents the design and measurement error analysis of a low-friction, lightweight linear SEA used in the Shipboard Autonomous Fire Fighting Robot (SAFFiR). The SAFFiR SEA pairs a stand-alone linear actuator with a configurable compliant member. Unlike most electric linear actuators, this actuator does not use a linear guide, which reduces friction and weight. Unlike other SEAs which measure the force by measuring the spring deflection, a tension and compression load cell is integrated into the design for accurate force measurements. The configurable compliant member is a titanium cantilever with manually adjustable length. The final SEA weighs 0.82[kg] with a maximum force of 1,000[N]. The configurable compliant mechanism has in a spring constant range of 145-512[kN/m]. Having no linear guide and incorporating the load cell into the universal joint both introduce measurement errors. The length error across a parallel ankle joint is less than 0.015[mm] and the force measurement error is less than 0.25% of the actual force. Finally, several changes are suggested for the next iteration of the SEA to improve its usability on future robots.

1. INTRODUCTION

Series elastic actuators (SEAs) provide the ability to perform high-bandwidth force control by placing an elastic component in series with the output of a rigid actuator [1-4]. Since their introduction by Pratt, SEAs have been frequently used in legged robotic applications because they mimic the biomechanical structure of legged animals [5]. Force control allows a humanoid robot to better respond to the unexpected disturbances it will encounter in unstructured environments. The spring can also be used to absorb impacts and store energy, reducing external loads on the actuator. A good force-controlled actuator has low friction so that it can command small forces. Using a low-impedance SEA enables impedance control, where the actuator can emulate a virtual mass-spring-damper system [6]. An actuator with low impedance will be easily backdriveable. Though the SEA presented in this paper will be used as a part of a humanoid robot, lightweight SEAs have many other robotic and prosthetic applications [7,8]. In all these applications, a good SEA will have low friction and impedance.

The elasticity in a SEA plays a large role in determining its force-control capabilities. SEAs with less compliance behave more similarly to rigid, position-controlled actuators than high-compliance systems. A larger amount of elasticity makes stable force control easier to attain. Several groups have developed variable compliant mechanisms to adapt their SEAs [9,10]. Altering the spring constants in a SEA-driven humanoid will change the natural frequency for the leg motions, increasing and decreasing the natural walking speeds.

Parallel actuation across a joint allows for multiple actuators to simultaneously drive the same number of degrees of freedom. For a humanoid robot, this typically translates to jointly driving either a hip or ankle with the same number of actuators as degrees of freedom. This scheme is simplified from

the human musculoskeletal system, where numerous muscles span a single joint and work cooperatively to drive limb movement. Only a handful of humanoid platforms utilize parallel actuation. These parallel mechanisms are composed of rotary motors actuating a series of drives and linkages [11], cables spanning across a joint [12], or linear actuators cooperatively driving the same body [13]. Parallel mechanisms can provide benefits to the strength and accuracy of the joint while decreasing inertia of the leg. Using linear actuators to cooperatively drive a parallel mechanism will require more degrees of freedom at each actuator end.

The lower body of the Shipboard Autonomous Fire Fighting Robot (SAFFiR), seen in Figure 1A, uses ten linear SEAs [14]. The actuators, highlighted in red in Figure 1B, are distributed across the hips, knees, and ankles of both legs. The actuators crossing the hip and ankle joints are in a parallel configuration. Unlike most SEA designs, the compliant element is not integrated into the actuator. Instead, the configurable compliant beams, highlighted in gold in Figure 1B, are independent of the linear actuators so that the compliance can be changed quickly [15]. The actuators attach to the structure of SAFFiR through the compliant members. This separation allows for modifications to the actuator or configurable compliant member without necessitating changes to both.

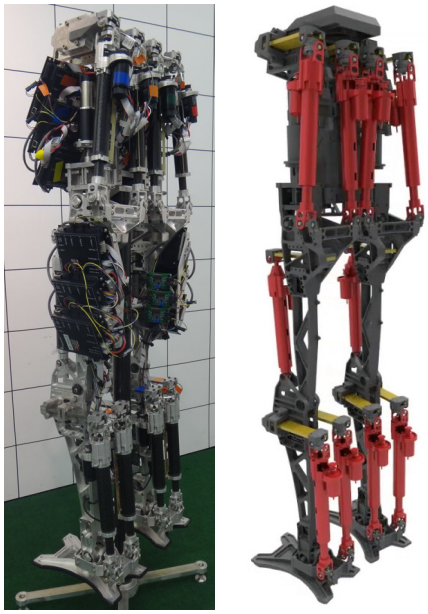

(A) (B)

Figure 1: (A) Lower body of SAFFiR and (B) render with actuators in red and configurable compliant beams in gold

Section 2 will outline the design of the linear SEA, including its specifications. The errors for the length and force measurements will be analyzed in Section 3. Section 4 will outline several design changes already underway for the next generation of the SEA. Section 5 will conclude the paper.

2. SERIES ELASTIC ACTUATOR DESIGN

The SEAs of SAFFiR have many novel features through their mechanical design. The SEA is comprised of two separable components: an electric linear actuator and a configurable compliant member. The actuators are lightweight and have low friction. There is a load cell integrated into each actuator, providing accurate direct force measurements. The actuators push against the configurable compliant members, which are attached to the structure of SAFFiR. The compliance at each joint can be tuned to match SAFFiR's walk. The detailed design of the actuators and the configurable compliant members are discussed below.

2.1 Linear Actuator Specifications

The actuators generate all the torque to move SAFFiR's legs. Lahr presents the design of SAFFiR in [14]. The actuators needed to produce at least 75[Nm] of torque at each joint in a nominal standing configuration, so the minimum peak force output is 1000[N]. Additionally, the actuators need to rotate each joint at a speed of 200[deg/s]. This correlates to the actuator having a minimum speed of 0.2[m/s]. These specifications led to the selection of several of the components of the actuator.

The motor that drives each actuator is a Maxon EC-4pole-30 brushless DC motor. Based on the motor's specifications, a 3.175[mm] pitch ballscrew was chosen. This ballscrew and motor pair needed a belt reduction between 2.5:1 and 4.375:1 in order to obtain the desired force and speed requirements. Because the maximum force requirement is only necessary in extreme circumstances like fall recovery with the limbs splayed, the actuators of SAFFiR are geared for speed with the 2.5:1 belt reduction.

2.2 Linear Actuator Design

A realistic rendering of the linear actuator is in Figure 2A and a rendering highlighting the ballscrew, ballnut, and cross gimbal with the load cell is in Figure 2B. The actuator attaches to a configurable compliance spring on the left of Figure 2A. This cantilever is attached to the structure of SAFFiR's leg. The connection to the spring is a universal joint (u-joint) with a non-intersecting axis gimbal highlighted in blue in Figure 2B. The gimbal of the u-joint has a uni-directional load cell built into the center for accurate force readings. A timing belt connects the brushless DC motor to a precision rolled ballscrew, shown in red. The ballscrew drives a ballnut, shown in green, which is directly connected to the smaller diameter carbon fiber tube in black. There is no linear guide for the ballnut, allowing it to rotate about the primary axis of the ballscrew. At the end of the smaller carbon tube is another u-joint. This u-joint connects to the structure of the robot. The legs of SAFFiR constrain the motion of the actuators. There is a larger carbon fiber tube that provides some dust protection for the ballscrew. Finally, a circuit board with contact switches is mounted on the outside of the actuator.

(A)

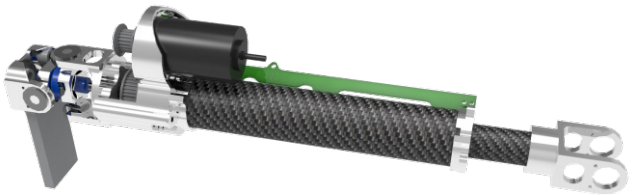

(B)

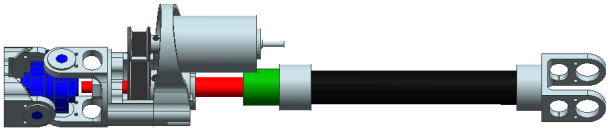

Figure 2: (A) Rendering of the linear series elastic actuator and (B) rendering highlighting the cross gimbal with the load cell, ballscrew, and ballnut

The linear actuator seen in Figure 2 is driven by either a 100[W] or 200[W] Maxon EC-4pole-30 motor at 48V. A 3.175[mm] pitch ballscrew is connected to the motor with a 5:2 timing belt reduction. Using the 100[W] motor results in a 0.653[kg] actuator capable of 300[N] of continuous force. A list of specifications for the 100[W] and 200[W] actuators can be seen in Table 1. The two motors are interchangeable without any mechanical modifications.

Table 1: SEA specifications

Actuator Type and Location	100[W] (Hip, Ankle)	200[W] (Knee)
Weight (Actuator Only) [kg]	0.653	0.735
Weight (Full SEA) [kg]	0.816	0.898
Maximum Speed [m/s]	0.35	
Length Range [m]	0.263 – 0.373	
Continuous Force [N]	300	500
Maximum Force [N]	1,000	1,600
Spring Constant [kN/m]	145– 512	

The smaller carbon fiber tube transfers the load from the ballscrew in the center of the actuator to the u-joint at the end of the actuator. This tube can be cut to any length between 0.018[m] plus the stroke of the actuator, where the fittings at the end of the tube physically intersect the ballscrew, and 0.59[m], where the tube will buckle at 1000[N]. The upper limit on length does not depend on the stroke of the actuator. The tube used on SAFFiR is 0.128[m] in order to cover the 0.11[m] stroke. This is enough stroke to create the necessary range of motion for SAFFiR.

A set of limit switches is mounted along the length of the actuator. They are physical-contact switches triggered by the ballnut. These switches are positioned at the center of the stroke and at 2[mm] before each end of the travel. The center limit switch on each actuator is used in the homing routine when the robot initializes. The switches are the only components that pass through the dust-protecting outer carbon fiber tube.

Two actuators cooperatively control two degrees of freedom at each of the hip and ankle joints, as seen in Figure 3. This parallel actuation scheme requires that one end of the actuator is a u-joint and the other is a spherical joint. In order to make the spherical joint, the actuator could have a traditional ball joint with a linear guide on the ballscrew, or it could have a u-joint with no linear guide.

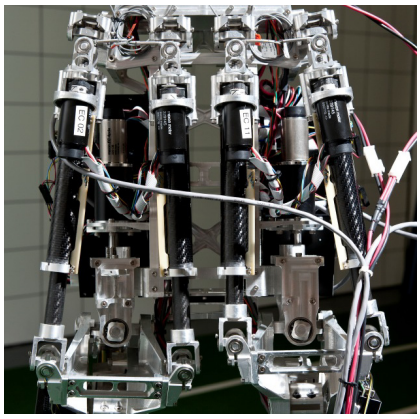

Figure 3: Two sets of parallel actuators spanning the hip joint

A linear guide would add weight and friction to the actuator. However, it would allow for a simple measurement of the absolute length of the actuator. Using a u-joint without a linear guide simplifies the design, reduces its weight, and reduces the overall friction in the actuator. But, the third degree of freedom in the spherical joint is achieved by allowing the ballnut to rotate, and not just translate, about the ballscrew axis. This rotation will result in an error in the length calculated from the quadrature encoder on the motor. For example, if the ballnut rotated 180° clockwise relative to the ballscrew, the length calculated from the encoder would be too short by 1.5875[mm]. There would be no sensors on the actuator to measure the ballnut rotation. The length measurement error will be discussed in Section 3.1. Because there are ten actuators on the robot, the actuator was designed with no guide to save weight.

An added benefit of eliminating the linear guide is decreasing the friction of the actuator. Even a well-designed linear guide system will introduce some friction to the actuator, reducing the minimum controllable force. Because the friction is low, the actuator is easily backdriveable by hand, making it easy to reposition SAFFiR while it is unpowered.

The actuator is intended to bolt onto a configurable compliance spring. To compensate for the spring constant uncertainty, it has a proprioceptive tension and compression Futek LCM200 load cell for direct force measurements. The load cell is highlighted in blue in Figure 2A. This load cell will measure up to 1100[N] in tension or compression. Building the load cell into the actuator allows for adjusting the compliance while minimally altering any of the control code. To reduce the length and weight of the actuator, the load cell is integrated into the gimbal of the u-joint. Placing the load cell in the gimbal will result in a reading error as the u-joint rotates due to the small axial misalignment of the load cell and the ballscrew. This force measurement error will be discussed in Section 3.2.

In order to tension the belt between the motor and ballscrew, the motor is mounted on an eccentric rotating disk as seen in Figure 4. Rotating the eccentric motor mount, the drive pulley can be moved closer to the ballscrew to get the belt over the pulley flange. Rotating the drive pulley away from the ballscrew tensions the timing belt.

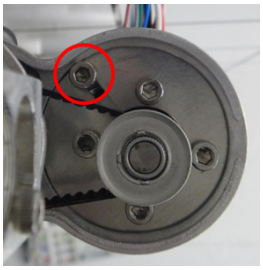

Figure 4: Eccentric motor mount with the tensioning bolt circled in red.

The motor mount is held in place by expanding to apply pressure to the surrounding material. The bolt circled in red in Figure 4 pulls a tapered plug into the mounting disk, forcing the disk to expand. This expansion applies pressure to the material surrounding the disk, holding it in place. A slit cut into motor mount decreases its rigidity, allowing the tapered plug to expand the disk outwards. A larges drawback to this tensioning method is that it is difficult to assemble with one person.

This method for holding the motor in place decreases the overall profile of the motor mounting mechanism while increasing the rigidity of the mounting structure compared to clamping around the motor mounting disk. The previous iteration of the actuator used an exterior clamp. Based on the location of the clamping bolt, the motor mount would deflect under high loads. The expanding disk method leaves enough support material so that the motor mount stays stationary.

2.3 Configurable Compliant Spring Design

SAFFiR uses a configurable compliant spring in series with the linear actuators. Machined out of titanium, the spring has a configurable range of spring constants between 145 and 512[kN/m]. Titanium provides a lightweight material with low amounts of hysteresis. The length of the spring cantilever is set before operating the robot and cannot be changed during use. The configurable compliant mechanism is shown in Figure 5.

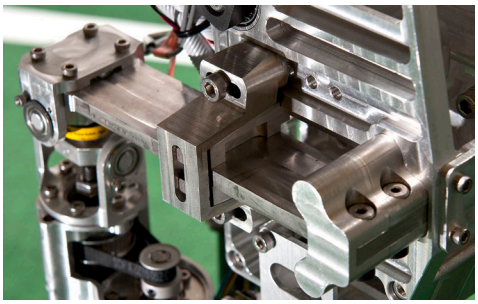

Figure 5: Configurable compliant mechanism

The configurable compliant mechanism interfaces directly with the structure of SAFFiR. The root of the cantilever beam is fixed against parts of the legs or torso. Farther down the length of the beam, a pair of square steel pins clamps on the titanium beam, creating a pseudo-fixed point in the middle of the beam. This clamping mechanism is shown in Figure 6. The pins, shown in black, are pressed into tapered pieces of aluminum, pictured in green. When loose, the tapered piece with the pins slide along the length of the cantilever, increasing and decreasing the spring constant while moving closer to and farther from the actuator respectively. Tightening down an outer tapered piece, shown in blue, pushes the pins against the compliant beam, using the pressure against the taper to hold the pins in place. The outer piece does not bottom-out against the structure of the robot, but instead is fastened when the pins firmly clamp the beam. The pins fit into a rectangular hole in the outer piece, aligning the tapered surfaces. The portion of the cantilever between the pins and root does not move while the section between the pins and actuator flexes in bending. The actuator attaches at the end of the cantilever by bolting into four threaded-inserts pressed into the titanium.

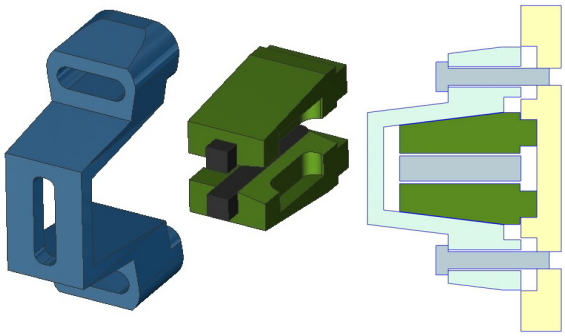

(A) (B)

Figure 6: Configurable compliance clamping mechanism. (A) Tapered pieces that lock around the titanium beam and (B) Rendering of the tapered pieces clamping the cantilever

The configurable compliance allows for tuning the springs to the walking of the robot. With the same mechanism, it is easy to test different stiffness settings at each leg joint. Additionally, the ankles can have looser compliance than the knees and hips which will aid the walking performance. One consequence of the configurable compliance is that it is difficult to accurately measure the spring constants of the cantilevers. Using calipers generates a good estimate, but not as exact as if the compliance was fixed at each joint. Furthermore, there is no guarantee that the compliance is configured identically for both actuators at the same parallel joint. Both of these drawbacks would make locomotion extremely difficult, so the actuator was designed with an integrated load cell.

3. ACTUATOR ERROR ANALYSIS

As discussed in Section 2, there are two known sources of measurement error. The length change calculated from the

motor encoder counts will be offset because there is no linear guide on the ballnut. The force measured by the load cell will be skewed because it is integrated into the cross gimbal of the u-joint. This section will address both sources of error.

Both length and force measurements are used in the overall control architecture of SAFFiR. During operation, the lengths of the actuators are used to calculate the positions of each joint. This is due to a lack of absolute encoders at each joint. The force measurements are used to calculate the joint torques, which are especially important while walking.

The error analysis will focus on the actuators of the ankle joint shown in Figure 7. Because of symmetry, the analysis will focus only on the actuator on the outside of the left ankle. The range of the ankle joint is ±40° in pitch and ±20° in roll. The axes for both pitch and roll are highlighted in Figure 7. It is assumed that the gimbal containing the load cell has intersecting axes and the configurable compliant member does not deflect to simplify all calculations.

Both analyses will be performed by comparing the three coordinate frames of the actuator seen in Figure 8 and Figure 9: the ballscrew in red, the ballnut in green, and the cross gimbal housing the load cell in blue. In Figure 8, both z-axes from the ballscrew and ballnut coordinate frames point into the page. This implies that the x-axis of the ballscrew frame is pointing upwards in the image, and the y-axis is pointing to the right. Likewise, the ballscrew and gimbal x-axes point out of the page in Figure 9. The z-axis of the ballscrew frame is pointing upwards and the y-axis is pointing to the right. This makes all three sets of axes align if the actuator is perfectly vertical and has no ballnut rotation.

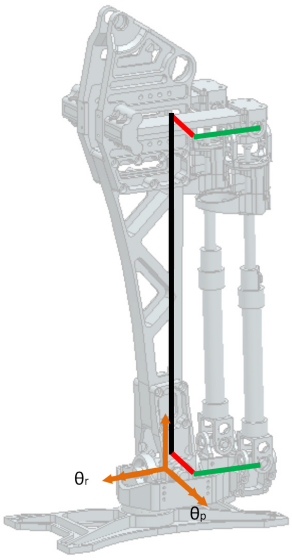

Figure 7: Ankle used in error analyses. The three dimensions used are in black, red, and green. The orange coordinate axes show the pitch and roll axes.

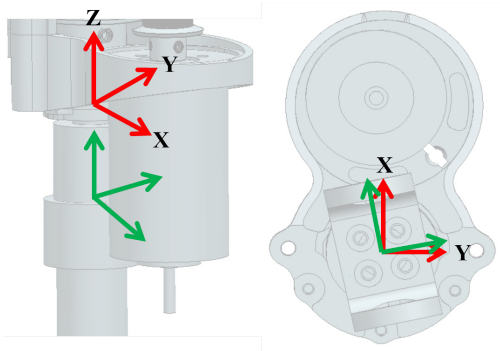

Figure 8: (A) Side view of ballscrew and ballnut frames and (B) Bottom projection of coordinate frames

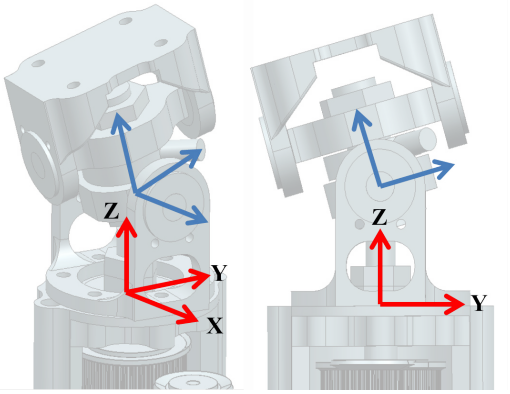

Figure 9: (A) Side view of ballscrew and gimbal frames and (B) Front projection of coordinate frames

As the robot moves, the coordinate frames move as well. Relative to the ballscrew coordinate frame, the ballnut frame can both translate and rotate about its z-axis. There is effectively a screw joint connecting those coordinate frames. The length error is calculated by comparing the angle between the x-axes of the ballscrew and ballnut coordinate frames. The gimbal frame rotates about its x-axis relative to the ballscrew frame. The force error is calculated by comparing the angle between the z-axes of the ballscrew and gimbal frames.

3.1 Length Measurement Error

The length error is calculated using the coordinate frames attached to the ballscrew and the ballnut. If there was a linear guide attached to the ballnut, the coordinate frames would always be translations of one another resulting in no length measurement error. However, due to the design of the actuator, the ballnut frame can rotate about the axis of the ballscrew.

The actuator can be represented as a vector spanning the ankle joint connecting the mounting points on the shin and foot. The exact vector can be solved for in both the coordinate frame of the shin, as seen in Equation 1, and the foot, as seen in Equation 2. The shorthand notations for $\sin(\theta)$ and $\cos(\theta)$ are $s\theta$ and $c\theta$ respectively.

$$\overrightarrow{r_{act,s}} = \begin{bmatrix} l_x\left(-1+c\theta_p\right) \\ l_x s\theta_r s\theta_p + l_y\left(1-c\theta_r\right) \\ -l_x c\theta_r s\theta_p - l_y s\theta_r + l_s \end{bmatrix}_{shin} \quad (1)$$

$$\overrightarrow{r_{act,f}} = \begin{bmatrix} l_x\left(1-c\theta_p\right)+l_y s\theta_r s\theta_p - l_s c\theta_r s\theta_p \\ l_y\left(-1+c\theta_r\right)+l_s s\theta_r \\ -l_x s\theta_p - l_y s\theta_r c\theta_p + l_s c\theta_r c\theta_p \end{bmatrix}_{foot} \quad (2)$$

The variables θ_p and θ_r are the joint angles of the ankle in pitch and roll respectively. The mounting offsets for the actuator from the center of the shin are l_x and l_y, colored in Figure 7 as green and red respectively. The vertical distance from the actuator mounting point to the ankle joint is l_s, shown in black. The length values can be seen in Table 2. The actuators are vertical when the ankle is in a neutral position, so l_x and l_y are the same for the shin and the foot. Equations 1 and 2 are related through a coordinate rotation of θ_p about the y-axis followed by a rotation of θ_r about the x-axis.

Table 2: Length values for the error analysis

l_x [m]	0.0722
l_y [m]	0.0388
l_s [m]	0.325

The vectors representing the actuator do not give enough information to actually compute the coordinate frames of the ballscrew and ballnut. The actuator vectors are just the z-axes of those coordinate frames. Each end of the actuator has a pitch and roll u-joint. The rotation angles of each u-joint are needed to solve for the ballscrew and ballnut coordinate frames. Rotating the z-axis of the shin coordinate frame first about the y-axis by φ_p and then the x-axis by φ_r will produce the actuator vector seen in Equation 1. Likewise, rotating the z-axis of the foot frame first about the x-axis by ψ_r and then the y-axis by ψ_p will produce the actuator vector in Equation 2. By equating the terms of the rotation matrices with the actuator vectors, the solutions for φ_p, φ_r, ψ_r, and ψ_p can be found in Equations 3-6 respectively. The values of φ_p, φ_r, ψ_r, and ψ_p are the rotations of the u-joints at each end of the actuator for a given θ_p and θ_r.

$$\varphi_p = s^{-1}\left(\frac{l_x\left(-1+c\theta_p\right)}{\left\|\overrightarrow{r_{act,s}}\right\|}\right) \quad (3)$$

$$\varphi_r = s^{-1}\left(\frac{-l_x s\theta_r s\theta_p - l_y\left(1-c\theta_r\right)}{\left\|\overrightarrow{r_{act,s}}\right\| c\varphi_p}\right) \quad (4)$$

$$\psi_r = s^{-1}\left(\frac{l_y\left(1-c\theta_r\right)-l_s s\theta_r}{\left\|\overrightarrow{r_{act,f}}\right\|}\right) \quad (5)$$

$$\psi_p = s^{-1}\left(\frac{l_x\left(1-c\theta_p\right)+l_y s\theta_r s\theta_p - l_s c\theta_r s\theta_p}{\left\|\overrightarrow{r_{act,f}}\right\| c\psi_r}\right) \quad (6)$$

Using φ_p, φ_r, ψ_r, and ψ_p, the two coordinate frames attached to the ballscrew and ballnut can be calculated. Transforming the frame attached to the ballnut into the shin frame leads to the rotation of the ballnut relative to the ballscrew. The coordinate frame attached to the ballscrew is already calculated in the shin coordinate frame. Multiplying the offset angle between the coordinate frames by the pitch of the ballscrew and dividing by a full rotation solves for the length error in the actuator. These results are in Figure 10. The ankle pitch rotation θ_p is on the x-axis in degrees, the roll rotation θ_r is on the y-axis in degrees, and the vertical axis represents the length error in [mm].

The results show that there will be a length error unless either θ_p or θ_r equals 0. However, looking closer reveals that the length error never exceeds ±0.015[mm]. This amount of error is within the machining tolerances of the parts of the actuator, so it will not affect the walking algorithm any more than the construction of the robot.

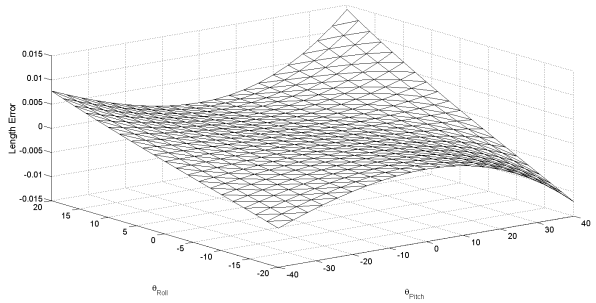

Figure 10: Length measurement error in the linear actuator

3.2 Force Measurement Error

The force error is calculated by comparing the coordinate frames of the ballscrew and the cross gimbal containing the load cell. When the load cell is axially aligned with the ballscrew, the load cell reading will exactly match the force of the actuator. However, when the two coordinate frames are not aligned, then the load cell reading represents a percentage of the actual force output. The non-axial component of the force causes bending in the load cell, generating incorrect force readings. This bending can also damage the load cell if it is too large.

Based on the design of the actuator, the angle between the ballscrew and the load cell axis is φ_r. The analytical solution for φ_r is in Equation 4. The percentage of the actual actuator force measured by the load cell is $\cos(\varphi_r)$, as shown in Figure 11. The

ankle rotation θ_p is on the x-axis in degrees, the rotation θ_r is on the y-axis in degrees, and the vertical axis represents the percentage of the actuator force measured by the load cell.

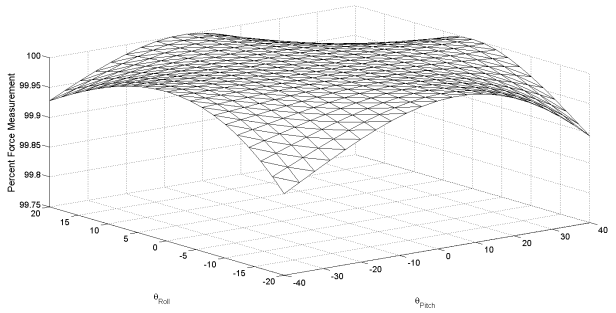

Figure 11: Percent of the actual force measured because the load cell is in the cross gimbal

The results show that the force reading stays within 99.75% of the true actuator force over the range of motion of the ankle. An interesting thing to note is that the force measurement matches the true force when θ_p equals zero, but not necessarily when θ_r equals zero. The gimbal containing the load cell rotates relative to the ballscrew when the ankle makes roll movements.

These analyses of the error in the ankle actuators validate the design decision to not have a linear guide. The maximum length error is 0.015[mm] and the load cell measures at least 99.75% of the actual force. This analysis is about the ankle joint, which resembles the joint actuation structure of most parallel-actuated humanoids. Analyzing the errors about SAFFiR's hip joint may have different results, due to a different range of motion. That investigation is left for future analysis.

The actuators were used to demonstrate walking with the SAFFiR platform. Lahr shows the results of the walking tests in [14]. SAFFiR is currently undergoing testing to develop force controlled walking and balancing algorithms which require the actuator load cell measurements.

4. FUTURE ACTUATOR CHANGES

There are several changes that will be made to the next generation of this SEA. Most of the changes will occur on the linear actuator in preparation for its use on the Tactical Hazardous Operations Robot (THOR), a disaster response robot. Both SAFFiR and THOR need to operate in harsh environments, so their actuators need to work reliably. Many of these changes will add weight and complexity to the design of the SEA, but will benefit the repeated operation of the robots.

The first change that will happen is shielding the moving components from dust and dirt. The motor drive belt is currently exposed to the environment. Adding a cap over the belt will provide some environmental protection at the cost of weight. Due to the design of the limit switches, there are holes in the actuator exposing parts of the ballscrew. Any amount of dirt in the ballscrew will affect the performance of the actuator through friction and potentially binding of the ballnut. Redesigning the limit switches to be either non-contact or small enough to fit inside the carbon fiber tube will allow for better protection of the ballscrew.

An absolute linear encoder will enable more-accurate control over the robot. As seen in Figure 10, there is some length error associated with the design of the actuator when it spans parallel joints. THOR will have a larger range of motion than SAFFiR, which may cause larger length measurement errors. An absolute encoder will mitigate this source of error.

As shown in Figure 11, the load cell is not always axially aligned with the ballscrew. This places the load cell under bending, which is not ideal for a uni-directional sensor. Moving the load cell out of the cross gimbal will improve the reliability of the measurements, but it can also add weight and length.

Designing a higher force actuator will be necessary for larger, more powerful robots. Increasing the belt ratio between the motor and ballscrew and by decreasing the pitch of the ballscrew will increase the output force. The high force actuator is estimated to produce about 3,000[N] with a 200[W] motor by changing the belt ratio and ballscrew pitch. Some of the components in the actuator, most notably the bearings, need to be changed to accommodate the higher forces. The bearings in the u-joints of the current SEA are rated for 1,000N each. This would have a factor of safety less of 0.67 at the highest load. This maximum force is also too large for the current load cells to measure.

The configurable compliant members do not need as large of a range of spring constants. By using different spring constant ranges at each joint determined through SAFFiR's walking testing, the compliant range will be better suited for operation. This will decrease the volume needed for the stiffer configurable compliant members at the hips and knees because the titanium beams will be shorter.

5. CONCLUSIONS

This paper presented the design and measurement error analysis of a lightweight, low friction linear SEA. The SEA pairs a stand-alone linear actuator with a configurable compliant member. The actuator is built without a linear guide, decreasing weight and friction while introducing error to the overall system. The configurable compliant mechanism can be manually set at each joint to better match the walking characteristics of SAFFiR. The load cell built into the actuator provides accurate force measurements regardless of the compliance configuration.

The design of the SEA naturally produces some measurement error in its length and force output because of its mechanical design, but it has been shown that those errors are small. The lengths of the ankle actuators stay within 0.015[m] of their calculated lengths. The readings from the load cell remain within 99.75% of the actual actuator forces. This level of error is acceptable for SAFFiR's walking algorithms.

Though this SEA is designed for humanoid robotics, it could be used in other applications. It is lightweight, low-friction, and backdriveable. However, some changes will

improve the usability of the next SEA. These improvements are already underway for the next generation design.

ACKNOWLEDGMENTS

This work is supported by ONR through grant N00014-11-1-0074 and by DARPA through grant N65236-12-1-1002. The authors would like to thank the reviewers for their valuable feedback.

REFERENCES

[1] Pratt, G. and Williamson, M., "Series Elastic Actuators". Proceedings of the IEEE International Conference on Intelligent Robots and Systems, Vol. 1, pp. 399-406, 1995.

[2] Pratt, J. and Krupp, B., "Series Elastic Actuators for Legged Robots". Proceedings of SPIE Unmanned Ground Vehicle Technology VI, Vol. 5422, pp. 135-144, 2004.

[3] Pratt, J., Krupp, B., and Morse, C., "Series Elastic Actuators for High Fidelity Force Control". Industrial Robot: an International Journal, Vol. 29, No. 3, pp. 234-241, 2002.

[4] Robinson, D., Pratt, J., Paluska, D., and Pratt, G., "Series Elastic Actuator Development for a Biomimetic Walking Robot". Proceedings of the IEEE/ASME International Conference on Advanced Intelligent Mechatronics, pp. 561-568, 1999.

[5] Pratt, G., "Low Impedance Walking Robots". Integrative and Comparative Biology, Vol. 42, Iss. 1, pp. 174-181, 2002.

[6] Pratt, G., Willisson, P., Bolton, C., and Hofman, A., "Late Motor Processing in Low-Impedance Robots: Impedance Control of Series Elastic Actuators". Proceedings of the 2004 American Control Conference, Vol. 4, pp. 3245-3251, 2004.

[7] Hollander, K., and Sugar, T., "Design of Lead Screw Actuators for Wearable Robotic Applications". Proceedings of the ASME International Design Engineering Technical Conferences & Computers and Information in Engineering Conference, Vol. 7, pp. 237-246, 2005.

[8] Hollander, K., Ilg, R., Sugar, T., and Herring, D., "An Efficient Robotic Tendon for Gait Assistance". ASME Journal of Biomechanical Engineering, Vol. 128, pp. 788-791, 2006.

[9] Hurst, J., Chestnutt, J., and Rizzi, A., "The Actuator With Mechanically Adjustable Series Compliance". IEEE Transactions on Robotics, Vol. 26, No. 4, pp. 597-606, 2010.

[10] Van Ham, R., Sugar, T., Vanderborght, B., Hollander, K., and Lefeber, D., "Compliant Actuator Designs". IEEE Robotics and Automation magazine, pp. 81-94, Sep. 2009.

[11] Lohmeier, S., Buschmann, T., and Ulbrich, H., "Humanoid Robot LOLA". Proceedings of the IEEE Conference on Robotics and Automation, pp. 775-780, 2009.

[12] Oort, G., Reinink, R., and Stramigioli, S., "New Ankle Actuation Mechanism for a Humanoid Robot". Preprints of the 18th IFAC World Congress, pp. 8082-8088, 2011.

[13] Pratt, J., and Krupp, B., "Design of a Bipedal Walking Robot". Proceedings of SPIE Unmanned Systems Technology X, Vol. 6962, 2008.

[14] Lahr, D., Orekhov, V., Lee, B., and Hong, D., "Development of a Parallelly Actuated Humanoid, SAFFiR". ASME International Design Engineering Technical Conferences & Computers and Information in Engineering Conference, 2013.

[15] Orekhov, V., Lahr, D., Lee, B., and Hong, D., "Configurable Compliance for Series Elastic Actuators". ASME International Design Engineering Technical Conferences & Computers and Information in Engineering Conference, 2013.